RAA 2020 Vol. **20** No. **2**, 16(10pp) doi: 10.1088/1674–4527/20/2/16

http://www.raa-journal.org *http://iopscience.iop.org/raa*

Research in Astronomy and Astrophysics

The kinematical and space structures of IC 2391 open cluster and moving group with Gaia-DR2

E. S. Postnikova[1], W. H. Elsanhoury[2,3], Devesh P. Sariya[4], N. V. Chupina[1], S. V. Vereshchagin[1] and Ing-Guey Jiang[4]

[1] Institute of Astronomy of Russian Academy of Sciences (INASAN), 48 Pyatnitskaya st., Moscow, Russia
[2] Astronomy Department, National Research Institute of Astronomy and Geophysics (NRIAG) 11421, Helwan, Cairo, Egypt (Affiliation ID: 60030681)
[3] Physics Department, Faculty of Science and Arts, Northern Border University, Turaif Branch, Saudi Arabia
[4] Department of Physics and Institute of Astronomy, "National Tsing Hua University", Hsinchu 30013; *deveshpath@gmail.com*

Received 2019 June 18; accepted 2019 August 20

Abstract The kinematical parameters, spatial shape and structure of the open cluster IC 2391 and the associated stellar stream are studied here using Gaia Data Release 2 (GDR2) astrometry data. The apex positions are determined for the open cluster IC 2391 (data taken from Cantat-Gaudin et al.) and for the kinematical stream's stars mentioned in Montes et al. employing both convergent point and AD-diagram methods. The values of apex coordinates are: $(A, D)_{\rm CP} = (6\overset{\rm h}{.}17 \pm 0\overset{\rm h}{.}004, -6\overset{\circ}{.}88 \pm 0\overset{\circ}{.}381$; for cluster) and $(6\overset{\rm h}{.}07 \pm 0\overset{\rm h}{.}007, -5\overset{\circ}{.}00 \pm 0\overset{\circ}{.}447$; stream), and $(A_0, D_0) = (6\overset{\rm h}{.}12 \pm 0\overset{\rm h}{.}004, -3\overset{\circ}{.}4 \pm 0\overset{\circ}{.}3$; cluster) and $(6\overset{\rm h}{.}21 \pm 0\overset{\rm h}{.}007, -11\overset{\circ}{.}895 \pm 0\overset{\circ}{.}290$; stream). The results are in good agreement with the previously calculated values. The positions of the stars in the disk and the spatial dispersion velocities are determined. The paths of cluster and associated stream are traced in the disk by orbit calculation back in time to their places of formation. A possible genetic relationship between the cluster and stream has been detected. The approximation of the spatial and kinematical shape of the stream and the cluster is made. According to this study, even though currently the cluster and stream seem to have a spatial difference in their locations, they appear to have formed in the same region of the Galactic disk.

Key words: Stars: kinematics and dynamics — Galaxy: stellar content — (Galaxy:) open clusters and associations: individual: IC 2391

1 INTRODUCTION

Stellar moving groups are ensembles of gravitationally unbound stars traveling with almost identical space motions (Montes et al. 2001, Chumak & Rastorguev 2006). IC 2391 is an interesting target which represents an open cluster as well as a stellar moving group (a.k.a. stream, flow or supercluster). The young moving group IC 2391 was discovered by Eggen (1991). In the Gaia era, with the availability of extremely precise data, moving groups are seeing new limelight to understand the Galactic disk in the solar neighborhood. Also, young clusters like IC 2391 in the solar vicinity enable us to characterize the abundance of our immediate portion of the Galactic disk (D'Orazi & Randich 2009).

IC 2391 (other names: MWSC 1529, Cl VDBH 42, omi Vel Cluster, C 0838-528, Escorial 31) is a nearby young open star cluster located south of the Galactic plane ($\alpha_{2000} = 08^{\rm h}40^{\rm m}32\overset{\rm s}{.}0$, $\delta_{2000} = -53^\circ02^{\rm m}00^{\rm s}$) with Galactic coordinates $(l, b) = (270\overset{\circ}{.}3622, -06\overset{\circ}{.}8387)$.

Due to its proximity, richness and low reddening, the cluster is well-studied in a wide range of frequencies from X-ray (Marino et al. 2005a), optical (Pagano et al. 2009), infrared (e.g., Siegler et al. 2007, Parker & Tinney 2013) to radio (Lim et al. 1996). IC 2391 is known to harbor stars which have just arrived on the zero age main sequence (Marino et al. 2005a). The cluster consists of stars with spectral types ranging from B to M which makes it interesting for studies of fast rotators (Marino et al. 2005b). The cluster is expected to have lost a significant amount of its population via evaporation caused by dynamical processes (Boudreault & Bailer-Jones 2009).

The cluster's heliocentric distance has been studied by various authors over the years. Efremov et al. (1997) re-

ported a Hipparcos (ESA 1997)-based distance modulus of IC 2391, $(m - M)$=5.84. Using Hipparcos data for 11 stars, Robichon et al. (1999) obtained a distance of 146^{+48}_{-45} pc. Dodd (2004) evaluated the cluster's distance as 147 ± 5.5 pc. Barrado y Navascués et al. (2004) determined an age of 50 Myr for IC 2391 from the excess of lithium in the atmospheres of stars. Platais et al. (2007) published a slightly lower value (40 Myr) for its age applying main-sequence fitting. IC 2391 is known to have a low reddening value, $E(B-V) = 0.01$ (Randich et al. 2001).

The proper motion of the cluster was stated by Loktin & Beshenov (2003) as ($\mu_\alpha \cos\delta, \mu_\delta = -25.05 \pm 0.34, 22.65 \pm 0.28$ mas yr^{-1}), while Dodd (2004) gave mean proper motion components $= -25.04 \pm 1.53$ and 23.19 ± 1.23 mas yr^{-1}. Both of these works used the Tycho-2 Catalogue (Høg et al. 2000). Dias et al. (2002) listed the values of the proper motion components as -24.97 ± 0.30 and 22.70 ± 0.30 mas yr^{-1}. The radial velocity of IC 2391 is 12.487 ± 3.533 km s^{-1} as reported by Conrad et al. (2014) and about 14.49 ± 0.14 km s^{-1} according to Dias et al. (2002).

In the three-dimensional (3D) velocity space, a kinematical stream (or moving group) of several dozens of stars is associated with the IC 2391 open cluster. Eggen (1991) discovered the stream and used the term "supercluster" for it. Montes et al. (2001) prepared a modern list of the member stars of the IC 2391 stream. The visible dimensions of the stream (in V) are $60'.00 \times 60'.00$. The member stars of the stream occupy a broad area of the sky, with its stars being scattered almost throughout the northern hemisphere. Eggen (1991, 1995) suggested an age spread among the stream's stars. Montes et al. (2001) provided an age estimate of 35 Myr for the stream.

With its unprecedentedly high accuracy, the Gaia data allow us to address the question of the reliability of the joint origin and the possible spatial-kinematic connection of the star stream and cluster. In this paper, we considered two lists of stars: cluster members of IC 2391 listed in Cantat-Gaudin et al. (2018) and another list of stars belonging to the stream from Montes et al. (2001). Data for the cluster and the stream's stars can be found in Table 1 and Table 2, respectively. We will utilize these parameters to determine apex positions (example, Vereshchagin et al. 2014; Elsanhoury et al. 2016, 2018) for the cluster and the stream using both the convergent point (CP) method and AD-diagram method. We also study the space motion, velocity ellipsoids, the shape in space and birthplaces for both cluster and stream.

The structure of this article is as follows: Section 2 explains the data used in this study. Section 3 deals with the kinematical properties. The next section describes velocity ellipsoid parameters (VEPs). In Section 5, we discuss the cluster's shape in space. Section 6 gives the birthplaces of the IC 2391 cluster and stream. The conclusions of this work are presented in Section 7.

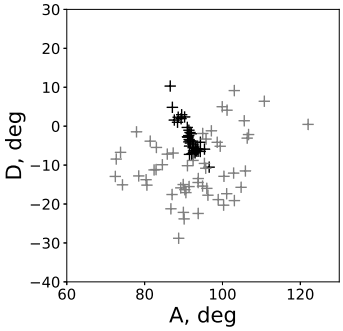

Fig. 1 The AD-diagram for IC 2391 open cluster and stream. *Black crosses* represent data for 39 cluster stars from Cantat-Gaudin et al. (2018) and the data for the stellar stream from Montes et al. (2001) are signified by *gray crosses*. The data for the stream contain 56 entries considering that some stars could be double or binary stars.

2 DATA AND SAMPLE OF STARS

Using Gaia Data Release 2 (GDR2, Gaia Collaboration et al. 2016, 2018) data, Cantat-Gaudin et al. (2018) provided a list of 224 probable members of IC 2391. Out of those, 39 stars have available radial velocity information. This list of 39 stars is considered in this paper for the analysis of IC 2391 cluster's kinematics. The data utilized for cluster stars are listed in Table 1.

The distances to the stars are determined by the parallaxes (π) from GDR2. For each measurement of π, the Monte Carlo method generated N random variables in the range of ($\pi \pm \sigma_\pi$). The resulting distribution is Gaussian with a maximum at a point with an argument value of π. Artificially modeled parallax values are transformed to distances according to the formula $1/\pi$, where π is specified in arcseconds. The distribution of the obtained distances is not normal. By the method of least squares, it is approximated by a curve representing a Maxwell distribution. The argument values corresponding to the maximum of this curve (maximum probability density) are regarded as the most likely distance values.

The list of stream stars was taken from Montes et al. (2001) and is shown in Table 2. The astrometric data (parallaxes and proper motion values) were referenced from GDR2 for most of the stars. For two stars (HIP IDs 11072 and 62686), the astrometric data were adopted from van Leeuwen (2007).

Tables 1 and 2 are compiled in a slightly different format: in Table 1 the first column gives GDR2 number, while the first two columns in Table 2 represent Hipparcos (HIP) and GDR2 numbers. Then, the tables contain parallaxes (π) and their errors; proper motion components (μ_α, μ_δ)

Table 1 Data for 39 Stars in IC 2391 Cluster

GDR2	$\alpha_{J2015.5}$ (deg)	$\delta_{J2015.5}$ (deg)	π (mas)	σ_π	μ_α (mas yr^{-1})	σ_{μ_α}	μ_δ (mas yr^{-1})	σ_{μ_δ}	V_r (km s^{-1})	σ_{V_r}	A (deg)	D (deg)	d (pc)
5317423293481147264	131.89258	–54.48348	6.55	0.02	–25.28	0.05	23.66	0.04	12.86	2.16	91.38	–1.04	151.65
5317884439832479872	130.75151	–53.90202	6.38	0.03	–23.29	0.06	22.85	0.06	16.48	4.82	94.29	–6.48	155.07
5317887321743547264	130.57572	–53.90217	6.64	0.04	–24.63	0.06	23.31	0.06	16.12	0.68	93.10	–6.34	148.84
5317906155187202176	130.34457	–53.63577	6.53	0.02	–24.91	0.04	23.20	0.05	16.51	1.32	92.58	–6.38	152.00
5318059532750974720	129.84384	–53.91815	6.48	0.05	–24.45	0.10	23.44	0.11	16.94	0.94	92.95	–6.86	151.61
5318069604459639552	129.10085	–54.01815	6.47	0.02	–23.69	0.04	23.38	0.05	14.11	2.21	91.02	–2.74	153.43
5318077507199948672	129.46469	–53.76262	6.68	0.02	–24.73	0.04	23.76	0.04	14.86	0.80	91.36	–4.04	148.63
5318093243960659456	130.20441	–53.62916	6.71	0.02	–24.04	0.04	23.80	0.04	13.55	0.61	91.99	–1.96	147.95
5318097916884923520	130.07602	–53.50790	6.60	0.02	–23.75	0.04	22.46	0.04	14.52	2.49	91.78	–4.32	150.34
5318150349846655488	128.93185	–53.35554	6.34	0.28	–24.26	0.53	23.51	0.50	17.61	7.77	92.55	–6.79	141.98
5318162238316886528	129.74460	–53.32008	6.60	0.02	–24.90	0.04	23.00	0.04	16.87	11.83	92.27	–7.11	150.20
5318170828251553792	129.31320	–53.33834	6.58	0.01	–24.02	0.03	23.07	0.03	9.66	12.47	87.13	4.84	151.29
5318176875565072768	129.22895	–53.14275	6.71	0.02	–23.96	0.05	23.78	0.04	16.20	1.52	93.07	–5.74	147.95
5318185667356683392	129.48414	–52.95143	6.66	0.03	–23.73	0.05	23.74	0.05	11.05	5.75	89.51	2.94	148.52
5318186221414047104	129.59528	–52.94657	6.66	0.02	–25.24	0.05	24.23	0.04	15.43	0.71	91.67	–3.76	148.91
5318229274167094656	131.56346	–53.75616	6.65	0.03	–24.66	0.05	22.92	0.04	16.00	0.83	93.73	–6.46	149.00
5318267653995965568	131.04233	–53.72592	6.68	0.03	–25.05	0.05	23.87	0.05	12.63	1.28	90.96	–0.33	148.43
5318296275658773888	131.44960	–53.43063	6.71	0.03	–26.09	0.05	23.48	0.05	15.83	8.73	92.44	–5.54	147.70
5318328676892604800	131.36203	–52.86715	6.65	0.02	–25.58	0.05	23.42	0.04	11.48	1.97	89.35	1.93	149.08
5318474941990522368	130.35768	–53.37808	6.65	0.03	–25.04	0.05	25.06	0.04	20.72	11.17	96.58	–10.53	149.08
5318504426950057728	130.49085	–52.87044	6.58	0.03	–25.73	0.05	22.70	0.05	17.12	2.11	92.07	–7.22	150.46
5318521671232021632	131.10882	–52.70888	6.58	0.03	–24.87	0.05	23.38	0.04	13.84	2.47	91.66	–1.62	150.78
5318532189619619328	130.98653	–52.68479	6.68	0.09	–22.95	0.16	22.84	0.14	14.84	3.70	94.33	–4.13	145.82
5318536999982933248	130.82442	–52.60302	6.52	0.03	–24.65	0.05	22.76	0.05	14.15	1.45	91.32	–2.43	151.65
5318541982138813824	129.99375	–53.05061	6.61	0.04	–25.30	0.07	24.69	0.07	17.24	0.83	93.48	–5.86	149.03
5318545521198976000	129.97087	–52.96569	6.56	0.02	–24.35	0.04	23.90	0.04	16.85	1.66	93.65	–5.87	151.25
5318546139674245888	129.92918	–52.96414	6.64	0.03	–25.44	0.05	22.48	0.05	16.78	2.79	91.52	–7.25	149.37
5318546822567826944	130.06753	–52.94134	6.54	0.03	–23.22	0.04	23.23	0.04	7.14	5.52	86.58	10.31	151.57
5318549678727766656	130.29139	–52.90283	6.58	0.03	–25.68	0.05	22.85	0.06	11.52	13.40	87.63	1.57	150.76
5318565656005527936	129.76157	–52.71059	6.50	0.02	–23.71	0.05	23.82	0.05	11.82	3.91	90.27	2.36	152.49
5318567958108066944	130.00665	–52.70338	6.64	0.03	–24.57	0.06	23.38	0.05	15.65	0.49	92.38	–4.63	149.21
5318647466543875584	131.91069	–52.26934	6.95	0.09	–25.41	0.16	24.42	0.18	16.68	2.97	95.37	–5.90	139.45
5321176205843037440	128.55421	–52.97214	6.70	0.02	–24.41	0.04	24.29	0.04	15.12	1.26	91.44	–3.43	148.14
5321188953307253760	129.35248	–52.90294	6.54	0.02	–23.94	0.05	22.51	0.05	15.50	4.71	91.55	–5.11	151.52
5321275295028390912	128.57546	–52.26594	6.44	0.02	–23.47	0.04	23.07	0.04	14.90	0.59	91.11	–2.80	153.80
5321280728169745536	128.75480	–52.23363	6.83	0.02	–24.52	0.04	24.36	0.04	17.26	2.55	93.34	–6.39	145.36
5321517672922567040	127.18998	–52.09067	6.42	0.02	–23.03	0.04	23.05	0.04	12.65	1.79	88.45	1.00	154.60
5321600445535344000	129.65022	–52.11067	6.63	0.03	–24.97	0.05	23.59	0.04	11.74	6.47	88.62	2.30	149.66
5321723109802924416	130.91001	–51.50794	6.54	0.05	–25.61	0.06	23.41	0.06	16.05	1.57	92.33	–3.85	150.41

The star list is taken from Cantat-Gaudin et al. (2018). Apex positions and distances mentioned in the table are determined in this paper.

and their errors. The next columns show radial velocities (V_r) and their errors. The references for the radial velocity data are mentioned in the "Ref." column (Table 2 only). For Table 1, all the values of radial velocity are taken from Cantat-Gaudin et al. (2018). The tables also present the values of apex (determined from AD-method) for individual stars determined in this work (A, D) and heliocentric distances (d).

Montes et al. (2001) originally presented a list of 53 stars for the stream associated with IC 2391. But, while cross-matching the data with GDR2, it gave us two entries in GDR2 for some stars. This is why Table 2 has 57 entries for stars. In the case of these stars, for the same HIP IDs, there were different GDR2 IDs. The fact that both the entries for these stars have approximately the same astrometric parameters supports the notion in favor of them being likely double or binary stars. The double star with two entries HIP 99803 was previously known, while the stars with Hipparcos IDs HIP 10175, 12326, 15058 and 42253 are new likely double or binary stars. For the star with HIP ID 15058, one of the entries had no available measurement for the radial velocity and its error. This limited our calculations for apex to 56 entries.

Owing to its better spatial resolution and overall superior characteristics, Gaia results are overtaking the Hipparcos ones in their scientific significance. This also means that in the regions where HIP could discover one star, Gaia may discover multiple stars. Although we are listing the stars with multiple entries as likely double or binary stars, we are not absolutely making claims about their status as double stars. The close values of astrometric parameters motivated us include these stars into our list rather than discarding such stars entirely or choosing one of the two entries.

3 KINEMATICAL PROPERTIES

3.1 Apex (vertex position) of the Cluster

Table 2 Data listed for star stream in Montes et al. (2001) cross-matched with other data sources to obtain astrometric parameters and radial velocities. Apex positions mentioned in the table are determined in this paper.

HIP	GDR2	π (mas)	σ_π (mas)	μ_α (mas yr^{-1})	σ_{μ_α}	μ_δ (mas yr^{-1})	σ_{μ_δ}	V_r (km s^{-1})	σ_{V_r}	Ref.	A (deg)	D (deg)	d (pc)
4979	2538159890494125184	16.95	0.07	122.91	0.15	–40.36	0.07	5.6	2.90	b	96.27	–17.73	58.44
6869	2593154747696080640	19.39	0.06	112.68	0.11	–33.45	0.12	8.61	0.16	a	91.00	–10.16	51.19
10175*	77161217776670208	23.32	0.06	113.92	0.11	–72.09	0.10	25.09	0.21	a	72.47	–12.91	42.64
10175*	77161222072044288	23.26	0.05	111.01	0.09	–73.34	0.09	22.6	2.00	c	74.31	–15.07	42.78
11072	–	45.53	0.82	196.61	0.81	–4.98	0.58	16.7	0.10	d	89.28	–15.85	21.07
12326*	4741722617241539456	17.04	0.16	64.82	0.29	54.02	0.28	13.63	1.20	a	81.44	–3.85	57.43
12326*	4741722823399969536	17.28	0.03	74.68	0.05	48.74	0.05	16.45	0.24	a	84.56	–9.90	57.66
12926	1145754724617168 64	39.60	0.06	237.61	0.09	–149.01	0.09	14.01	0.15	a	95.98	–15.98	25.17
13081	1148326207437358 08	43.41	0.04	279.96	0.08	–119.15	0.06	10.21	0.21	a	105.89	–11.52	22.99
14150	1153114580580614 40	47.16	0.06	233.12	0.12	–168.44	0.12	10.09	0.13	a	100.29	–20.30	21.15
14954	3265335443260522112	44.37	0.20	193.25	0.32	–69.29	0.31	19.62	0.15	a	94.88	–15.39	22.31
15058*	3266941481859767680	13.79	0.13	80.89	0.18	–9.32	0.22	–	–	a	–	–	71.00
15058*	3266941486151475456	14.98	0.23	72.09	0.30	–15.07	0.39	28.3	0.20	b	87.33	–6.90	64.42
22449	3288921720024442496	124.35	0.39	462.10	0.75	12.13	0.57	22.54	3.76	a	110.75	6.40	7.98
23200	3231945508509506176	40.98	0.03	39.23	0.06	–95.05	0.04	18.08	0.63	a	88.74	–28.80	24.36
25119	3234412606443085824	50.39	0.11	64.45	0.32	–180.09	0.24	36.30	0.24	a	89.96	–22.15	19.74
29241	2912022740481002752	17.68	0.03	–28.65	0.04	45.06	0.05	26.98	0.19	a	77.91	–1.46	56.31
33690	5479222240596469632	54.47	0.02	–162.07	0.05	264.64	0.04	22.04	0.19	a	80.38	–13.75	18.34
40774	3089675232224086784	44.66	0.04	–164.23	0.07	–53.49	0.05	27.35	0.17	a	92.44	–8.80	22.34
42253*	666296182348971776	25.45	0.04	–110.14	0.07	–102.81	0.04	23.13	0.56	a	93.78	–13.46	39.15
42253*	666296212412465024	25.54	0.04	–108.78	0.07	–102.91	0.05	19.30	0.29	a	90.61	–17.07	39.00
47193	1144716265940854016	3.72	0.29	–16.79	0.61	–17.61	0.50	–6.98	0.10	e	98.90	–18.87	265.11
50371	5253347574048995584	4.34	0.39	–23.92	0.63	6.73	0.63	8.06	1.15	a	85.82	–7.18	225.37
50660	749024502373761664	20.64	0.08	–152.52	0.09	–58.66	0.08	2.88	0.40	a	80.59	–15.14	48.04
51931	3750851328223270400	31.36	0.07	–163.87	0.09	22.62	0.09	18.79	0.18	a	106.70	–2.15	31.74
52468	5254185333222868352	3.40	0.25	–14.70	0.43	2.28	0.41	9.1	0.30	b	90.33	–16.32	292.08
57198	4004885655800704896	3.94	0.07	–22.86	0.09	–7.49	0.08	5.14	0.28	a	102.86	–12.05	253.84
59280	1536064958579187840	39.82	0.06	–314.20	0.05	–51.00	0.07	–2.61	0.12	a	95.36	–9.57	25.03
60831	1541667932396172800	21.95	0.04	–182.13	0.04	–4.69	0.05	–2.21	0.18	a	95.77	–3.31	45.37
60832	1541667932396172416	21.94	0.04	–180.39	0.05	0.44	0.06	–1.91	0.19	a	94.92	–1.88	45.38
62686	–	26.13	3.38	–135.82	3.60	–27.22	5.02	–2.9	0.40	b	100.39	–12.89	27.23
62758	3958028490314315008	25.81	0.04	–141.07	0.06	–37.86	0.04	–4.24	0.23	a	101.08	–17.35	38.59
66252	3630092241022731136	48.73	0.06	–286.58	0.11	–91.87	0.08	–23.16	0.16	a	72.71	–8.44	20.46
67412	3658911226765436032	22.94	0.06	–136.86	0.09	–44.06	0.07	–13.44	0.25	a	91.41	–15.52	43.33
68076	1671816367861537408	21.75	0.03	–138.54	0.06	54.51	0.05	–15.12	0.14	a	89.90	–15.00	45.84
69713	1511727333122255744	34.30	0.18	–149.63	0.27	88.89	0.30	–18.4	2.70	b	78.48	–12.79	28.80
74045	1701849283160198400	33.76	0.15	–127.83	0.31	165.69	0.30	–8.72	0.77	f	83.02	–5.46	29.33
77152	1224551770875466496	20.67	0.05	–88.05	0.06	37.70	0.07	–20.5	0.35	a	98.64	–4.14	48.14
77749	4403292246725472384	24.59	0.04	–115.09	0.07	10.81	0.07	–24.90	0.14	a	99.94	5.00	40.52
84827	5811053234948685312	25.43	0.09	–47.08	0.13	–199.34	0.18	–3.30	0.20	a	93.73	–14.47	39.00
85360	5976271757721062528	21.94	0.07	–26.13	0.12	–109.38	0.09	–16.03	0.27	a	93.76	–22.43	45.28
89005	2260109892505203328	31.78	0.03	–26.17	0.06	194.87	0.06	–13.88	0.36	a	99.42	–5.16	31.40
90004	4153637759337630720	24.03	0.06	–23.10	0.09	–68.30	0.09	–25.52	0.14	a	104.78	–15.71	41.39
93096	6711686642605457408	13.53	0.04	24.30	0.06	–72.81	0.06	–12.82	0.40	a	87.04	–17.56	73.41
99803*	6468703708258513024	15.51	0.06	35.37	0.08	–98.19	0.07	–17.19	0.40	a	106.35	–3.07	63.93
99803*	6468703712555652096	15.45	0.05	37.07	0.08	–93.29	0.06	–19.67	0.44	a	105.59	1.39	64.26
101262	1863898674120773760	37.13	0.03	141.86	0.05	16.81	0.06	–26.72	0.17	a	90.15	–23.83	26.88
104225	2270771375724754816	31.00	0.03	108.41	0.05	66.26	0.05	–12.72	0.17	a	86.75	–21.23	32.20
105232	1846882224145757056	25.45	0.06	133.59	0.11	9.56	0.11	–16.92	0.26	a	82.42	–11.25	39.08
109110	2621051110038749440	27.45	0.05	176.76	0.09	–43.74	0.09	–11.31	0.63	a	82.93	–11.15	36.27
109612	6508969718149502976	20.45	0.03	114.74	0.06	–65.22	0.06	–9.78	0.35	a	97.15	–1.19	48.72
112909	1889703525209960960	66.42	0.07	523.78	0.10	–48.49	0.12	–2.78	0.55	a	73.81	–6.72	15.02
113556	2663025241307454848	4.53	0.06	39.39	0.08	–6.67	0.08	–16.28	0.78	a	95.69	–10.81	220.90
114236	6393744472971218048	17.80	0.04	103.61	0.05	–63.04	0.05	3.56	0.18	a	103.06	–19.12	55.92
115288	2818000408811106688	15.61	0.18	73.65	0.37	20.25	0.22	–19	4.40	b	121.99	0.46	62.40
116384	2646280705713202816	48.03	0.08	339.80	0.09	28.52	0.07	–10.44	0.52	a	101.16	4.10	20.74
117410	2420563960807395072	35.47	0.90	234.22	1.45	23.16	1.30	–9.88	0.95	a	103.04	9.14	26.58

This table has 57 entries (see Sect. 2). The values of parallaxes (π) and proper motions with their errors are referenced from GDR2. For the stars with no entries in GDR2 (with HIP numbers 11072 and 62686), the values and errors of π and proper motions are adopted from van Leeuwen (2007). Pairs of stars marked with an asterisk (*) near HIP number are considered likely double or binary stars. The "Ref." column contains the references for V_r and σ_{V_r} according to: a – GDR2, b – Gontcharov (2006), c – Wilson (1963), d – Tokovinin (2013), e – Famaey et al. (2005) and f – White et al. (2007).

It is known that a moving cluster is a group of stars whose parallel motions on the celestial sphere and its direction of proper motion will be directed towards a virtual point called CP or apex of this group. This method has been applied by our group to determine the apex and other kinematical parameters for open clusters M67, NGC 188 and

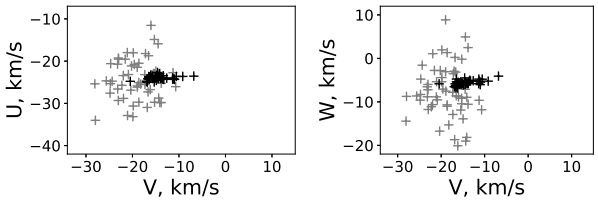

Fig. 2 Comparison of the spatial velocities of the stars in the cluster and the stream. The velocities are expressed in km s^{-1}. Cluster stars are signified in *black* and stream stars are represented in *gray*.

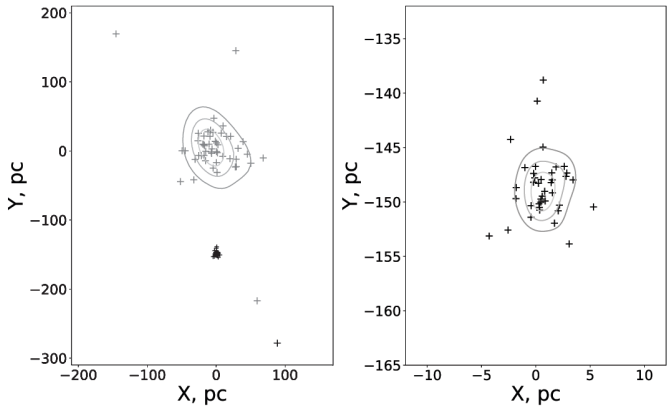

Fig. 3 The Galactic XY plane distribution is displayed here for the stream stars (Table 2, *gray crosses*) – left panel; and for the cluster stars of IC 2391 (Table 1, *black crosses*) – right panel. In the left panel, the stars in the cluster are also visible as a small agglomeration of *black crosses* at the lower side from the center of the stream stars' distribution. *Contours* signifying equal stellar flux density are drawn in the both panels.

the Pleiades (Vereshchagin et al. 2014, Elsanhoury et al. 2016, 2018).

Here, we calculate the apex for both cluster and stream represented by IC 2391 with the classical CP and AD-diagram methods.

3.1.1 The CP method

It is a classical method which depends on the components of the proper motion vectors (i.e., $\mu_\alpha \cos\delta$ and μ_δ in mas yr^{-1}). Also, implementing the well-known formulae given by Smart (1968), we can estimate the velocity components (V_x, V_y, V_z) along x, y and z-axes in the coordinate system centered at the Sun for a group of N cluster member stars with coordinates (α, δ), at distance r_i (pc) and with radial velocity V_r (km s^{-1}), i.e.,

$$V_x = -4.74 r_i \mu_\alpha \cos\delta \sin\alpha - 4.74 r_i \mu_\delta \sin\delta \cos\alpha + V_r \cos\delta \cos\alpha\,,$$
$$V_y = +4.74 r_i \mu_\alpha \cos\delta \cos\alpha - 4.74 r_i \mu_\delta \sin\delta \sin\alpha + V_r \cos\delta \sin\alpha\,,$$
$$V_z = +4.74 r_i \mu_\delta \cos\delta + V_r \sin\delta\,.$$

From the above equations and letting $\xi = \frac{V_x}{V_z}$, $\eta = \frac{V_y}{V_z}$, we get

$$a_i\xi + b_i\eta = c_i\,,$$

where the coefficients

$$a_i = \mu_\alpha^{(i)} \sin\delta_i \cos\alpha_i \cos\delta_i - \mu_\delta^{(i)} \sin\alpha_i\,,$$
$$b_i = \mu_\alpha^{(i)} \sin\delta_i \sin\alpha_i \cos\delta_i + \mu_\delta^{(i)} \cos\alpha_i\,,$$
$$c_i = \mu_\alpha^{(i)} \cos^2\delta_i\,,$$

and the index i varies from 1 to N which is the number of cluster members. So,

$$\tan A_{CP} = \frac{\eta}{\xi}\,, \qquad (1)$$

$$\tan D_{CP} = (\eta^2 + \xi^2)^{-1/2}\,. \qquad (2)$$

The coordinates (A_{CP}, D_{CP}) of the cluster apex are derived from Equations (1) and (2). The results on the apex position of both the cluster and the stream are presented in Table 3.

3.1.2 The AD-diagram method

The formulae to construct the AD-diagram can be seen in Chupina et al. (2001, 2006). The value of the apex coordinates for the IC 2391 cluster using data from Table 1 is (A_0, D_0)= ($6\overset{\text{h}}{.}12 \pm 0\overset{\text{h}}{.}004$, $-3\overset{\circ}{.}4 \pm 0\overset{\circ}{.}3$). For the stellar stream, using data from Table 2 the apex position is (A_0, D_0)= ($6\overset{\text{h}}{.}21 \pm 0\overset{\text{h}}{.}007$, $-11\overset{\circ}{.}895 \pm 0\overset{\circ}{.}290$). Figure 1 presents the constructed AD-diagrams for the cluster and stream. It

is evident that the directions of movement in space for the cluster and the stream almost coincide.

3.2 Space Velocity Components (U, V, W)

In order to compute the space velocity components U, V and W, we applied an equatorial-Galactic transformation explained in Liu et al. (2011). They determined the position of the Galactic plane utilizing recent catalogs like the Two-Micron All-Sky Survey (2MASS, Skrutskie et al. 2006) and defined the optimal Galactic coordinate system by adopting the ICRS position of the compact radio source Sagittarius A* at the Galactic center (Liu et al. 2011).

The values of space velocity components along the three axes are expressed as

$$U = -0.0518807421V_x - 0.8722226427V_y - 0.4863497200V_z\,,$$
$$V = +0.4846922369V_x - 0.4477920852V_y + 0.7513692061V_z\,,$$
$$W = -0.8731447899V_x - 0.1967483417V_y + 0.4459913295V_z\,.$$

Figure 2 depicts the components (U, V, W) of spatial velocities of the cluster stars and stream stars, for which the input data were taken from Tables 1 and 2. As can be seen in Figure 2, the components of space velocities of all the stars do not show much different orientation. Thus, it can be concluded that both the cluster and stream move in approximately the same direction.

4 VELOCITY ELLIPSOID PARAMETERS

4.1 Formulae for the Velocity Ellipsoid Parameters

To compute the velocity ellipsoid and its parameters for the IC 2391 open cluster and stream, we followed the computational algorithm mentioned in Elsanhoury et al. (2015). A brief explanation of the algorithm is given here.

The coordinates of the i^{th} star with respect to axes parallel to the original axes, but shifted to the center of the distribution, i.e., towards average velocities ($\overline{U}$, $\overline{V}$ and $\overline{W}$), will be $(U_i - \overline{U})$; $(V_i - \overline{V})$; $(W_i - \overline{W})$. The average velocities $\overline{U}$, $\overline{V}$ and $\overline{W}$ are defined as

$$\overline{U} = \frac{\sum_{i=1}^{N} U_i}{N},\ \overline{V} = \frac{\sum_{i=1}^{N} V_i}{N},\ \overline{W} = \frac{\sum_{i=1}^{N} W_i}{N}\,. \qquad (3)$$

N is the total number of stars.

Let ξ be an arbitrary axis with its zero point coincident with the center of the distribution, and let l, m and n be the direction cosines of the axis with respect to the shifted ones, then the coordinates Q_i of the point i, with respect to the ξ-axis are written as

$$Q_i = l(U_i - \overline{U}) + m(V_i - \overline{V}) + n(W_i - \overline{W})\,. \qquad (4)$$

If the measured scatter components are Q_i, a generalization of the mean square deviation can be defined as

$$\sigma^2 = \frac{1}{N}\sum_{i=1}^{N} Q_i^2. \qquad (5)$$

From Equations (3), (4) and (5) we deduce that $\sigma^2 = \underline{x}^T B \underline{x}$, where $\underline{x}$ is the (3×1) direction cosines vector and B is a (3×3) symmetric matrix with elements μ_{ij}

$$\mu_{11} = \tfrac{1}{N}\sum_{i=1}^{N} U_i^2 - (\overline{U})^2,\ \mu_{12} = \tfrac{1}{N}\sum_{i=1}^{N} U_iV_i - \overline{UV}\,,$$
$$\mu_{13} = \tfrac{1}{N}\sum_{i=1}^{N} U_iW_i - \overline{UW},\ \mu_{22} = \tfrac{1}{N}\sum_{i=1}^{N} V_i^2 - (\overline{V})^2\,,$$
$$\mu_{23} = \tfrac{1}{N}\sum_{i=1}^{N} V_iW_i - \overline{VW},\ \mu_{33} = \tfrac{1}{N}\sum_{i=1}^{N} W_i^2 - (\overline{W})^2\,.$$

The necessary conditions for an extremum are now

$$(B - \lambda I)\underline{x} = 0\,. \qquad (6)$$

These are three homogeneous equations in three unknowns, which have a nontrivial solution if and only if

$$D(\lambda) = |B - \lambda I| = 0\,, \qquad (7)$$

where λ is the eigenvalue, and $\underline{x}$ and B are written as

$$\underline{x} = \begin{bmatrix} l \\ m \\ n \end{bmatrix} \text{ and } B = \begin{bmatrix} \mu_{11} & \mu_{12} & \mu_{13} \\ \mu_{21} & \mu_{22} & \mu_{23} \\ \mu_{31} & \mu_{32} & \mu_{33} \end{bmatrix}.$$

Equation (7) is the characteristic equation for the matrix B. The required roots (i.e., eigenvalues) are

$$\lambda_1 = 2\,\rho^{\frac{1}{3}}\cos\tfrac{\phi}{3} - \tfrac{k_1}{3}\,,$$
$$\lambda_2 = -\rho^{\frac{1}{3}}\left(\cos\tfrac{\phi}{3} + \sqrt{3}\sin\tfrac{\phi}{3}\right) - \tfrac{k_1}{3}\,,$$
$$\lambda_3 = -\rho^{\frac{1}{3}}\left(\cos\tfrac{\phi}{3} - \sqrt{3}\sin\tfrac{\phi}{3}\right) - \tfrac{k_1}{3}\,,$$

where

$$k_1 = -(\mu_{11} + \mu_{22} + \mu_{33})\,,$$
$$k_2 = \mu_{11}\mu_{22} + \mu_{11}\mu_{33} + \mu_{22}\mu_{33} - \left(\mu_{12}^2 + \mu_{13}^2 + \mu_{23}^2\right),$$
$$k_3 = \mu_{12}^2\mu_{33} + \mu_{13}^2\mu_{22} + \mu_{23}^2\mu_{11} - \mu_{11}\mu_{22}\mu_{33} - 2\mu_{12}\mu_{13}\mu_{23}\,,$$
$$q = \tfrac{1}{3}k_2 - \tfrac{1}{9}k_1^2\,,\quad r = \tfrac{1}{6}(k_1k_2 - 3k_3) - \tfrac{1}{27}k_1^3\,,$$
$$\rho = \sqrt{-q^3}\,,\qquad x = \rho^2 - r^2\,,$$
$$\phi = \tan^{-1}\left(\tfrac{\sqrt{x}}{r}\right).$$

Depending on the matrix that controls the eigenvalue problem (Eq. (6)) for the velocity ellipsoid, we establish analytical expressions of some parameters for the correlations studies in terms of the matrix elements μ_{ij} of the eigenvalue problem for the velocity ellipsoid (i.e., VEPs).

4.1.1 The $\sigma_j, j = 1, 2, 3$ parameters

The $\sigma_j, j = 1, 2, 3$ parameters are defined as $\sigma_j = \sqrt{\lambda_j}$.

Table 3 Kinematical Parameters Determined in this Study for the IC 2391 Cluster and Star Stream

Parameters	Results	References
N	39	Table 1
N	56	Table 2
$(A, D)_{CP}$	$6\overset{\mathrm{h}}{.}17 \pm 0\overset{\mathrm{h}}{.}004$, $-6\overset{\circ}{.}88 \pm 0\overset{\circ}{.}381$	Table 1
	$6\overset{\mathrm{h}}{.}07 \pm 0\overset{\mathrm{h}}{.}007$, $-5\overset{\circ}{.}00 \pm 0\overset{\circ}{.}447$	Table 2
(A_0, D_0)	$6\overset{\mathrm{h}}{.}12 \pm 0\overset{\mathrm{h}}{.}004$, $-3\overset{\circ}{.}4 \pm 0\overset{\circ}{.}3$	Table 1
	$6\overset{\mathrm{h}}{.}21 \pm 0\overset{\mathrm{h}}{.}007$, $-11\overset{\circ}{.}895 \pm 0\overset{\circ}{.}290$	Table 2
	$5\overset{\mathrm{h}}{.}83$, $-12\overset{\circ}{.}44$	Montes et al. (2001)
	$5\overset{\mathrm{h}}{.}82$, $-12\overset{\circ}{.}44$	Eggen (1991)
$(\overline{U}, \overline{V}, \overline{W})$ km s^{-1}	$-23.634, -14.449, -5.525$	Table 1
	$-21.110, -7.213, -6.653$	Table 2
	$-20.6, -15.7, -9.1$	Montes et al. (2001)
(x_c, y_c, z_c) pc	$-57.84, 68.78, -119.66$	Table 1
	$4.471, -0.552, 9.287$	Table 2
Space velocity (km s^{-1})	28.25 ± 0.19	Table 1
$= \left(\overline{U}^2 + \overline{V}^2 + \overline{W}^2\right)^{1/2}$	23.28 ± 0.21	Table 2
	27.453 ± 5.24	Montes et al. (2001)
	30.00	Eggen (1991)
$(\lambda_1, \lambda_2, \lambda_3)$ km s^{-1}	$779.54, 4.83, 0.19$	Table 1
	$590.65, 44.06, 10.16$	Table 2
$(\sigma_1, \sigma_2, \sigma_3)$ km s^{-1}	$27.92, 2.20, 0.44$	Table 1
	$24.30, 6.64, 3.19$	Table 2
Dispersion velocity (km s^{-1})	28.11 ± 0.18	Table 1
	25.39 ± 0.20	Table 2
(l_1, m_1, n_1) deg	$0.83, 0.51, 0.20$	Table 1
	$0.89, 0.34, 0.30$	Table 2
(l_2, m_2, n_2) deg	$-0.53, 0.85, 0.01$	Table 1
	$-0.36, 0.13, 0.92$	Table 2
(l_3, m_3, n_3) deg	$0.16, 0.11, -0.98$	Table 1
	$0.28, -0.93, 0.24$	Table 2
L_j, $j = 1, 2, 3$	$-31\overset{\circ}{.}655, -121\overset{\circ}{.}757, 145\overset{\circ}{.}685$	Table 1
	$-20\overset{\circ}{.}941, -159\overset{\circ}{.}951, -106\overset{\circ}{.}453$	Table 2
B_j, $j = 1, 2, 3$	$11\overset{\circ}{.}286, 0\overset{\circ}{.}511, -78\overset{\circ}{.}702$	Table 1
	$17\overset{\circ}{.}490, 67\overset{\circ}{.}342, 13\overset{\circ}{.}946$	Table 2
$S_\odot$, km s^{-1}	28.25 ± 0.19	Table 1
	23.28 ± 0.21	Table 2
l_A	$-31\overset{\circ}{.}439$	Table 1
	$-18\overset{\circ}{.}866$	Table 2
b_A	$11\overset{\circ}{.}279$	Table 1
	$16\overset{\circ}{.}609$	Table 2

4.1.2 The l_j, m_j and n_j parameters

The l_j, m_j and n_j are the direction cosines for the eigenvalue problem. We have the following expressions for l_j, m_j and n_j as

$$l_j = \frac{\mu_{22}\mu_{33} - \sigma_i^2\left(\mu_{22} + \mu_{33} - \sigma_i^2\right) - \mu_{23}^2}{D_j},\ j = 1, 2, 3,$$
$$m_j = \frac{\mu_{23}\mu_{13} - \mu_{12}\mu_{33} + \sigma_j^2\mu_{12}}{D_j},\ j = 1, 2, 3,$$
$$n_j = \frac{\mu_{12}\mu_{23} - \mu_{13}\mu_{22} + \sigma_j^2\mu_{13}}{D_j},\ j = 1, 2, 3,$$

where

$$D_j^2 = \left(\mu_{22}\mu_{33} - \mu_{23}^2\right)^2 + \left(\mu_{23}\mu_{13} - \mu_{12}\mu_{33}\right)^2 + \left(\mu_{12}\mu_{23} - \mu_{13}\mu_{22}\right)^2 + 2[(\mu_{22} + \mu_{33})\left(\mu_{23}^2 - \mu_{22}\mu_{33}\right) + \mu_{12}\left(\mu_{23}\mu_{13} - \mu_{12}\mu_{33}\right) + \mu_{13}\left(\mu_{12}\mu_{23} - \mu_{13}\mu_{22}\right)]\sigma_j^2 + \left(\mu_{33}^2 + 4\mu_{22}\mu_{33} + \mu_{22}^2 - 2\mu_{23}^2 + \mu_{12}^2 + \mu_{13}^2\right)\sigma_j^4 - 2\left(\mu_{22} + \mu_{33}\right)\sigma_j^6 + \sigma_j^8\,.$$

Considering (x_c, y_c, z_c; pc) is the center of the cluster, it can be estimated as the equatorial coordinates of the center of mass for N number of discrete objects as given below

$$x_c = \frac{\sum_{i=1}^{N}\left(r_i \cos\alpha_i \cos\delta_i\right)}{N},$$
$$y_c = \frac{\sum_{i=1}^{N}\left(r_i \sin\alpha_i \cos\delta_i\right)}{N},$$
$$z_c = \frac{\sum_{i=1}^{N}\left(r_i \sin\delta_i\right)}{N}.$$

4.1.3 The L_j and B_j parameters

Let L_j and B_j, $j = 1, 2, 3$ be the Galactic longitude and Galactic latitude of the directions which correspond to the extreme values of the dispersion, then

$$L_j = \tan^{-1}\left(\frac{-m_j}{l_j}\right),\quad B_j = \sin^{-1}(-n_j)\,.$$

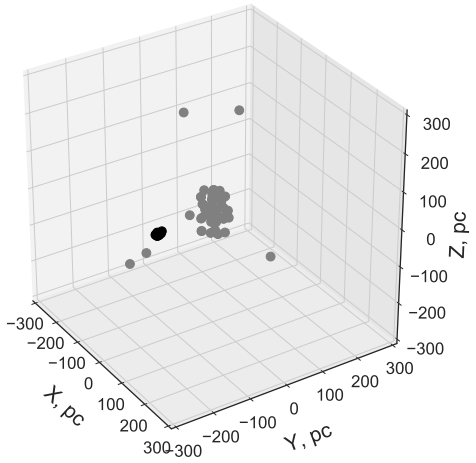

Fig. 4 The 3D picture of the cluster and stream stars in the rectangular Galactic coordinate system. The *black points* are cluster stars, while the *gray points* are stream stars.

4.1.4 The solar elements

The solar motion can be defined as the absolute value of the Sun's velocity relative to the group of stars under consideration, i.e.,

$$S_{\odot} = \left(\overline{U}^2 + \overline{V}^2 + \overline{W}^2\right)^{1/2}, \text{ km s}^{-1}.$$

The Galactic longitude l_A and Galactic latitude b_A of the solar apex are

$$l_A = \tan^{-1}\left(\frac{-\overline{V}}{\overline{U}}\right), \quad b_A = \sin^{-1}\left(\frac{-\overline{W}}{S_{\odot}}\right).$$

4.2 The Calculated VEPs

We have a distribution of residual velocities of stars inside the cluster and moving group. In Table 3 we present the results of our calculations.

5 THE CLUSTER'S AND STREAM'S SHAPES IN SPACE

In Figure 3, the curves show contours of equal star flux density. The kernel-density estimation was done considering Gaussian kernels (Scott 2015) using the SciPy Python package (Jones et al. 2001) to make the isodensity plot. At the periphery of the stream as well as the cluster, stars are so few that it is not possible to determine a significant value for density. As can be seen in Figure 3 (left panel), the stars from the stream occupy a region stretched roughly along (at a small angle not exceeding 40 deg) the axis OY. The axis OY represents the direction of Galactic rotation. The reason behind this orientation is the process leading to the decay of clusters (from the associations containing multiple clusters) with their gradual stretching (due to differential rotation) along the direction of rotation of the Galactic disk. This causes the gradual transformation of clusters into streams with their transformation into ordered ring structures stretched around the Galactic center (Perottoni et al. 2019; Wang et al. 2019). Interestingly, a similar distribution of stellar flows/streams is observed in other galaxies (Pearson et al. 2019). The fact that the stream's stars are scattered over a wide area of the sky and there are greater uncertainties in their selection makes the distribution of stream stars much more scattered than the cluster stars in Figure 3. As for the IC 2391 cluster itself, represented by a handful of stars (from Table 1) in Figure 3 (right panel), its spatial outline manifests the same pattern with a stretching along the OY direction. Since the number of stars in the sample used here is small, the structure is not defined in fine details.

Figure 4 features the 3D distribution of stars in the cluster and stream under consideration. It is noticeable from Figure 4 that the stars from the cluster and the stream are located in separate regions in space.

6 THE BIRTHPLACES OF THE IC 2391 STREAM AND OPEN STAR CLUSTER

Figure 5 exhibits the position of the stars in the cluster and the stream approximately at the time of their formation, as determined by trial calculations of orbits back in time, up to 70 million years ago. The galpy program was employed to calculate the orbits (Bovy 2015). Note that similar calculations carried out implementing another method are available in Kharchenko et al. (2009) and Chumak & Rastorguev (2006). Gravitational interactions among the stars in the stream were not taken into account. For the cluster, the effect of irregular forces was not considered (the dispersion of the peculiar velocities of stars is a neg-

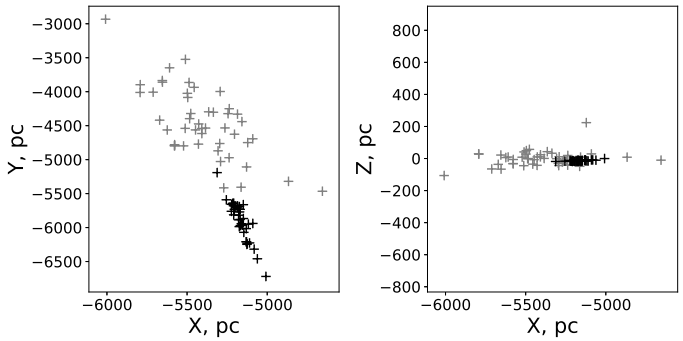

Fig. 5 Places of star formation for the cluster stars (*black crosses*, data from Table 1) and for the stream stars (*gray crosses*, Table 2).

ligible value compared with the spatial velocity). In addition, the calculations did not account for the effect of spiral arms. As suggested by Figure 5, we conclude that the birthplaces of the stars in the cluster and the stream are in the same region of the disk.

7 CONCLUSIONS

In this work, we have determined various kinematical parameters of the open cluster IC 2391 ($n = 39$ stars) and the associated stream ($n = 57$ stars). A computational routine using the "Mathematica" software has been developed to compute the kinematical structure.

We calculated the apex positions by two independent methods: CP method and AD-diagram applying the two data presented in Table 1 and Table 2. We have determined the apex position with CP method $(A, D)_{CP} = (6\overset{h}{.}17 \pm 0\overset{h}{.}004, -6\overset{\circ}{.}88 \pm 0\overset{\circ}{.}381$; for cluster) and $(6\overset{h}{.}07 \pm 0\overset{h}{.}007, -5\overset{\circ}{.}00 \pm 0\overset{\circ}{.}447$; for stream). We have also obtained the apex values from AD-diagram $(A_0, D_0) = (6\overset{h}{.}12 \pm 0\overset{h}{.}004, -3\overset{\circ}{.}4 \pm 0\overset{\circ}{.}3)$ and $(6\overset{h}{.}21 \pm 0\overset{h}{.}007, -11\overset{\circ}{.}895 \pm 0\overset{\circ}{.}290)$ for the cluster and the stream, respectively. Results from both the CP and AD-diagram methods are almost the same.

For the cluster IC 2391 and the stream, we have determined the VEPs, including velocity dispersion (σ_j), direction cosines l_j, m_j and n_j, Galactic longitude and latitude (L_j, B_j) with ($j = 1, 2, 3$), and solar elements $S_\odot$, l_A and b_A. The parameters of the ellipsoids of residual velocities (VEPs) for the stars in the cluster and the stream are also determined.

It is evident from the two-dimensional Figure 3 and the 3D structure of the cluster and the stream depicted in Figure 4 that the cluster and the stream are not spherically symmetric structures in Galactic space. They are elongated in shape and point along the direction of Galactic rotation. In general, all of this is consistent with the theoretical ideas regarding the tidal forces of the Galaxy acting on a stellar system, stretching the system towards the Galactic center, and the differential rotation of the Galactic disk, turning the system in the direction of rotation. In addition, we obtained evidence of the genetic connection between the star cluster IC 2391 and the stream back in time, leading to the time of their formation in the Galactic disk.

Acknowledgements We are thankful to the referee of this paper for useful and constructive comments. Devesh P. Sariya and Ing-Guey Jiang are supported by grants from the Ministry of Science and Technology (MOST), Taiwan (MOST 105-2811-M-007 -038, MOST 105-2119-M-007 -029 -MY3, MOST 106-2112-M-007 -006 -MY3 and MOST 106-2811-M-007 -051). This work has made use of data from the European Space Agency (ESA) mission *Gaia* [1], processed by the *Gaia* Data Processing and Analysis Consortium (DPAC[2]). Funding for the DPAC has been provided by national institutions, in particular the institutions participating in the *Gaia* Multilateral Agreement. This research has made use of the SIMBAD database, operated at CDS[3], Strasbourg, France, Wenger et al. (2000).

References

Barrado y Navascués, D., Stauffer, J. R., & Jayawardhana, R. 2004, ApJ, 614, 386

Boudreault, S., & Bailer-Jones, C. A. L. 2009, ApJ, 706, 1484

Bovy, J. 2015, ApJS, 216, 29

Cantat-Gaudin, T., Jordi, C., Vallenari, A., et al. 2018, A&A, 618, A93

Chumak, Y. O., & Rastorguev, A. S. 2006, Astronomy Letters, 32, 446

Chupina, N. V., Reva, V. G., & Vereshchagin, S. V. 2001, A&A, 371, 115

Chupina, N. V., Reva, V. G., & Vereshchagin, S. V. 2006, A&A, 451, 909

Conrad, C., Scholz, R.-D., Kharchenko, N. V., et al. 2014, A&A, 562, A54

Dias, W. S., Alessi, B. S., Moitinho, A., & Lépine, J. R. D. 2002, A&A, 389, 871

[1] *https://www.cosmos.esa.int/gaia*

[2] *https://www.cosmos.esa.int/web/gaia/dpac/consortium*

[3] *http://simbad.u-strasbg.fr/simbad/*

Dodd, R. J. 2004, MNRAS, 355, 959
D'Orazi, V., & Randich, S. 2009, A&A, 501, 553
Efremov, Y. N., Schilbach, E., & Zinnecker, H. 1997, Astronomische Nachrichten, 318, 335
Eggen, O. J. 1991, AJ, 102, 2028
Eggen, O. J. 1995, AJ, 110, 2862
Elsanhoury, W. H., Nouh, M. I., & Abdel-Rahman, H. I. 2015, RMxAA, 51, 199
Elsanhoury, W. H., Haroon, A. A., Chupina, N. V., et al. 2016, New Astron., 49, 32
Elsanhoury, W. H., Postnikova, E. S., Chupina, N. V., et al. 2018, Ap&SS, 363, 58
ESA 1997, The HIPPARCOS and TYCHO Catalogues, Astrometric and Photometric Star Catalogues Derived from the ESA HIPPARCOS Space Astrometry Mission, 1200
Famaey, B., Jorissen, A., Luri, X., et al. 2005, A&A, 430, 165
Gaia Collaboration, Prusti, T., de Bruijne, J. H. J., et al. 2016, A&A, 595, A1
Gaia Collaboration, Brown, A. G. A., Vallenari, A., et al. 2018, A&A, 616, A1
Gontcharov, G. A. 2006, Astronomy Letters, 32, 759
Høg, E., Fabricius, C., Makarov, V. V., et al. 2000, A&A, 355, L27
Jones, E., Oliphant, E., Peterson, P. et al. 2001, SciPy: Open Source Scientific Tools for Python (`http://www.scipy.org/`)
Kharchenko, N. V., Berczik, P., Petrov, M. I., et al. 2009, A&A, 495, 807
Lim, J., Slee, O. B., & Stauffer, J. R. 1996, in Astronomical Society of the Pacific Conference Series, 109, Cool Stars, Stellar Systems, and the Sun, eds. R. Pallavicini, & A. K. Dupree, 371
Liu, J.-C., Zhu, Z., & Hu, B. 2011, A&A, 536, A102
Loktin, A. V., & Beshenov, G. V. 2003, Astronomy Reports, 47, 6
Marino, A., Micela, G., Peres, G., Pillitteri, I., & Sciortino, S. 2005a, A&A, 430, 287
Marino, A., Micela, G., Peres, G., Pillitteri, I., & Sciortino, S. 2005b, in ESA Special Publication, 560, 13th Cambridge Workshop on Cool Stars, Stellar Systems and the Sun, eds. F. Favata, G. A. J. Hussain, & B. Battrick, 787
Montes, D., López-Santiago, J., Gálvez, M. C., et al. 2001, MNRAS, 328, 45
Pagano, I., Spezzi, L., Marino, G., et al. 2009, in American Institute of Physics Conference Series, 1094, 15th Cambridge Workshop on Cool Stars, Stellar Systems and the Sun, ed. E. Stempels, 951
Parker, S. R., & Tinney, C. G. 2013, MNRAS, 430, 1208
Pearson, S., Starkenburg, T. K., Johnston, K. V., Williams, B. F., & Ibata, R. A. 2019, arXiv:1906.03264
Perottoni, H. D., Martin, C., Newberg, H. J., et al. 2019, MNRAS, 486, 843
Platais, I., Melo, C., Mermilliod, J.-C., et al. 2007, A&A, 461, 509
Randich, S., Pallavicini, R., Meola, G., Stauffer, J. R., & Balachandran, S. C. 2001, A&A, 372, 862
Robichon, N., Arenou, F., Mermilliod, J.-C., & Turon, C. 1999, A&A, 345, 471
Scott, D. W. 2015, Multivariate Density Estimation: Theory, Practice, and Visualization (Hoboken, NJ: John Wiley and Sons)
Siegler, N., Muzerolle, J., Young, E. T., et al. 2007, ApJ, 654, 580
Skrutskie, M. F., Cutri, R. M., Stiening, R., et al. 2006, AJ, 131, 1163
Smart, W. M. 1968, Stellar kinematics (London: Longmans, 1968)
Tokovinin, A. 2013, AJ, 145, 76
van Leeuwen, F. 2007, A&A, 474, 653
Vereshchagin, S. V., Chupina, N. V., Sariya, D. P., Yadav, R. K. S., & Kumar, B. 2014, New Astron., 31, 43
Wang, H.-F., Huang, Y., Carlin, J. L., et al. 2019, arXiv:1905.11944
Wenger, M., Ochsenbein, F., Egret, D., et al. 2000, A&AS, 143, 9
White, R. J., Gabor, J. M., & Hillenbrand, L. A. 2007, AJ, 133, 2524
Wilson, R. E. 1963, General Catalogue of Stellar Radial Velocities (Washington: Carnegie Institute)